Journal of Hydrology 430–431 (2012) 173–178

Contents lists available at SciVerse ScienceDirect

Journal of Hydrology

journal homepage: www.elsevier.com/locate/jhydrol

Unsaturated properties for non-Darcian water flow in clay

Hui-Hai Liu *, Lianchong Li, Jens Birkholzer

Earth Science Division, Lawrence Berkeley National Laboratory, Berkeley, CA 94720, United States

ARTICLE INFO

Article history:
Received 18 August 2011
Received in revised form 25 January 2012
Accepted 7 February 2012
Available online 16 February 2012
This manuscript was handled by Philippe Baveye, Editor-in-Chief, with the assistance of Renduo Zhang, Associate Editor

Keywords:
Unsaturated flow
Clay rock
Non-Darcian flow
Geological repository
Shale gas

SUMMARY

Clay rock formations, and compacted clay (e.g., bentonite) used as backfill within disposal drifts, have been considered as natural and engineered barriers, respectively, for isolating high-level nuclear wastes in mined geologic repositories. Accurately modeling unsaturated flow in those clay materials is important for assessing the performance of a geological repository. While the non-Darcian behavior of water flow in clay materials has been demonstrated in the literature, a systematic study of modeling unsaturated non-Darcian flow is still lacking. Based on a hypothesis that pore water in clay becomes non-Newtonian as a result of water–clay interaction, we propose new constitutive relationships for unsaturated flow, including a relationship between water flux and hydraulic gradient and those among capillary pressure, water saturation, and hydraulic conductivity. An evaluation based on a set of laboratory experimental observations supports the usefulness of the proposed relationships. More experimental studies are desirable for further confirming the non-Newtonian water flow behavior in clay materials and evaluating the proposed relationships.

1. Introduction

Clay/shale formations have been considered as potential host rock for geological disposal of high-level radioactive waste because of its low permeability, low diffusion coefficient, high retention capacity for radionuclides, and capability to self-seal fractures. For example, Callovo-Oxfordian argillites at the Bure site, France (Fouche et al., 2004), Toarcian argillites at the Tournemire site, France (Patriarche et al., 2004), Opalinus Clay at the Mont Terri site, Switzerland (Meier et al., 2000), and Boom Clay at the Mol site, Belgium (Barnichon and Volckaert, 2003) have all been under intensive scientific investigation with field experiments conducted in underground research laboratories. These investigations, which also included laboratory experiments and modeling analyses, have focused on achieving a better understanding of a variety of rock properties and their relationships to flow and transport processes associated with geological disposal of radioactive waste.

In geologic repositories for radioactive waste disposal, compacted expansive clay soils (bentonites) are often considered as buffer materials within an engineered barrier system, to be placed in the repository tunnels between the radioactive waste and the host rock. The bentonite is usually compacted at low water content, and then progressively wetted by water from the surrounding host formation. As a result, an unsaturated zone generally develops within the near field of a clay repository. The unsaturated wetting process is accompanied by bentonite swelling which ensures acceptable sealing of open spaces between waste packages and the corresponding host formation. At the same time, heat emanating from the decaying radioactive waste causes thermal gradients and unsaturated flow within the engineered and natural barriers. Accurately modeling unsaturated flow in such clay materials, and how it is related to swelling and heat transfer processes, is critical for assessing the performance of both clay rock and buffer materials for isolating radioactive wastes at a disposal site.

It has been documented in the literature that water flow in clays cannot be adequately described by Darcy's law, which states that water flux is directly proportional to the hydraulic gradient. For example, Hansbo (2001) reported that water flux is proportional to a power function of the hydraulic gradient when the gradient is less than a critical value, whereupon the relationship between water flux and gradient becomes linear for large gradient values. He explained this behavior by positing that a certain hydraulic gradient is required to overcome the maximum binding energy of mobile pore water. In contrast, Dixon et al. (1999) presented measured hydraulic conductivity data for clays, finding no "critical" or "threshold" gradients from their observations. However, they did find that there were "transitional" gradients that define two separate regions of Darcian flow. Lower hydraulic conductivities were observed for hydraulic gradients less than the transitional gradient. Dixon et al. (1999) indicated that clay could contain considerable quantities of structured water that shears at gradients above the transitional gradient, allowing it to participate in advective flow. Finally, Zou (1996) proposed a nonlinear flux-gradient relationship depending on the activation energy of pore liquid. He assumed that the activation energy of pore water

* Corresponding author. Tel.: +1 510 486 6452; fax: +1 510 486 5686.
E-mail address: hhliu@lbl.gov (H.-H. Liu).

0022-1694/$ - see front matter © 2012 Elsevier B.V. All rights reserved.
doi:10.1016/j.jhydrol.2012.02.017

in clay (or other fine-grained materials) is not only variable with the distance from the solid particle surface, but also with the flow velocity of pore water. His model, including several empirical parameters, was able to fit a number of data sets that show nonlinear flux-gradient relationships at low hydraulic gradients and linear relationships at high gradients. More studies of non-Darcian behavior for water flow in clay can be found in references cited in Hansbo (2001), Dixon et al. (1999), and Zou (1996). Although some inconsistency seems to exist among these studies, in general these studies demonstrated the existence of non-Darcian flow behavior in clay under conditions of relatively low hydraulic gradients.

Note that such studies are all for saturated flow conditions. It is expected that non-Darcian flow behavior becomes more significant under unsaturated conditions, because in such conditions, pore water exists as water films or occurs in relatively small pores, and therefore should be subject to relatively strong interactions with the clay surface. (As reported in Low (1961), soil–water properties change as a result of the interactions including hydration and double-diffusive-layer effects.) This seems to be supported by experimental observations recently reported by Cui et al. (2008). They observed non-Darcian behavior for the full range of observed hydraulic gradients under unsaturated conditions.

While several models have been proposed for describing non-Darcian flow in clay in saturated conditions, a systematic investigation of constitutive models for unsaturated flow in clay materials is still lacking. The objective of this work is to develop such a model under unsaturated conditions, by considering pore water as a non-Newtonian fluid.

2. Theoretical model

This section presents a theoretical model describing non-Darcian flow under unsaturated conditions. The model will be verified in the next section with data from a laboratory experiment. Theoretical development of the model is based on the hypothesis that pore water in clay materials is non-Newtonian and that flow is driven by the hydraulic gradient.

2.1. Newtonian and non-Newtonian fluids

In general, fluids can be classified as Newtonian or non-Newtonian. The former has a constant viscosity; thus, its shear stress is directly proportional to the shear rate defined as the velocity gradient perpendicular to the plane of shear. For non-Newtonian fluid, the viscosity is not constant anymore, but rather a function of shear rate and/or time. For example, Fig. 1 shows typical relations between shear stress and shear rate for a Newtonian fluid and three non-Newtonian fluids. Pseudoplastic or shear-thinning fluids have a lower apparent viscosity at higher shear rates, and dilatant, or shear-thickening fluids increase in apparent viscosity at higher shear rates (e.g., Wu and Pruess, 1998). Bingham plastic fluids have a linear shear stress/shear strain relationship and require a finite yield stress before they begin to flow. In other words, the plot of shear stress against shear strain does not pass through the origin (Fig. 1).

A relatively simple way to describe non-Newtonian behavior is to express the apparent viscosity (μ_e) as a power function of shear rate $\frac{\partial u}{\partial y}$ (e.g., Christopher and Middleman, 1965):

$$\mu_e = \kappa\left(\frac{\partial u}{\partial y}\right)^{n-1} \tag{1}$$

where κ is a constant, u is water velocity parallel to the plane of shear, y is a coordinate perpendicular to the plane of shear, and n is a dimensionless number. The corresponding fluids are called

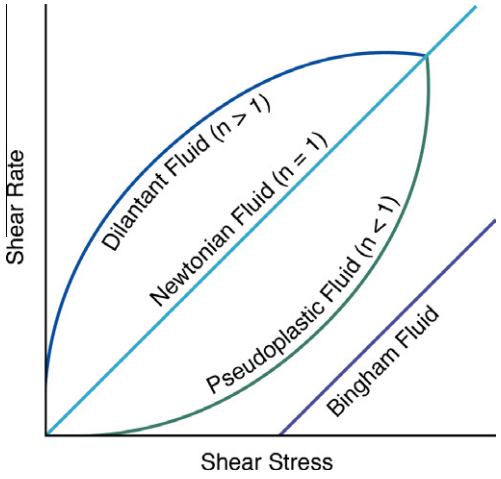

Fig. 1. Schematic demonstration of relations between shear stress and stress rate for a Newtoniain fluid and three typical non-Newtonian fluids.

"power-law fluids". In this case, the shear stress of fluid, τ, is given by

$$\tau = \mu_e\left(\frac{\partial u}{\partial y}\right) = \kappa\left(\frac{\partial u}{\partial y}\right)^n \tag{2}$$

Eqs. (1) and (2) correspond to pseudoplastic fluids ($n < 1$), Newtonian fluids ($n = 1$), and dilatant fluids ($n > 1$), respectively. In this study, we focus on power-law fluids following Eqs. (1) and (2); Bingham plastic fluid is not considered. As demonstrated below, these equations seem to capture the non-Darcian behavior of pore water under unsaturated conditions reasonably well. Note that the methodology developed in this study can be easily applied to Bingham plastic fluids as well, when needed.

It is well documented in the literature that water properties will change near the clay surface as a result of water–clay interaction. Like other researchers (e.g., Zou, 1996), we believe that the observed non-Darcian behavior for water flow is caused by non-Newtonian properties of pore water in clay materials. These properties should be a direct result of strong water–clay interaction. However, this argument is largely based on observations at core scales, and to the best of our knowledge has not been directly confirmed by measured viscosity and shear-rate data at pore scale. Thus, at this point, it is appropriate to treat the considered correlation between non-Darcian behavior and non-Newtonian properties as a hypothesis.

2.2. Relationship between flux and hydraulic gradient for a capillary tube

In this subsection, we derive a relationship between water flux and hydraulic gradient for a capillary tube with radius R (Fig. 2). This will be used as the basis for developing corresponding relationships for clay materials. For simplicity, we consider a horizontal capillary tube here, although this relationship could easily be extended to capillary tubes with other orientations.

Considering water to be a non-Newtonian fluid in the capillary tube and using Eqs. (1) and (2), we can write the shear-stress relationship as

$$\tau = \kappa\left(\left|\frac{du}{dr}\right|\right)^n \tag{3}$$

where r is the radius coordinate. For a water surface with radius r and length dx (Fig. 2), the total shearing force is

$$F = \tau(2\pi r)dx \tag{4}$$

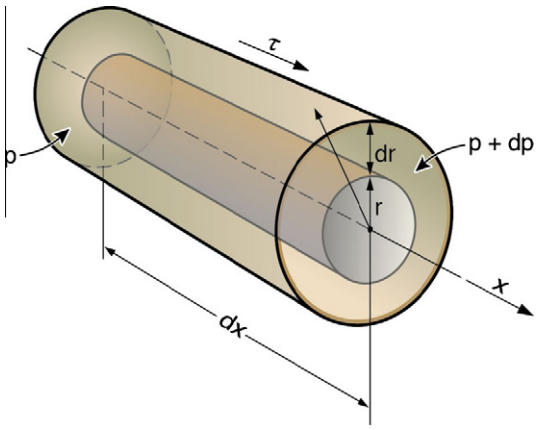

Fig. 2. A water element in a capillary tube with radius R. The variable r is the radius of a water element within the capillary tube and ranges from zero to R.

Then, the net shearing force for a water element with thickness dr within the capillary tube, dF, is given by $dF = 2\pi(dx)d(r\tau)$. For laminar flow, the inertial effect can be ignored. In this case, the shearing force should be balanced by an opposing pressure on the water element that is $(dp)(dr)(2\pi r)$. Therefore, we have:

$$dF = 2\pi(dx)d(r\tau) = (dp)(dr)(2\pi r) \tag{5}$$

Combining (3)–(5) yields:

$$r\frac{dp}{dx} = \frac{d(r\tau)}{dr} = \frac{d(r\kappa\left[\left|\frac{du}{dr}\right|\right]^n)}{dr} \tag{6}$$

The above equation can be solved for shear rate (or velocity gradient $\frac{du}{dr}$)

$$\frac{r^2}{2}\frac{dp}{dx} + C = \kappa r(\left|\frac{du}{dr}\right|)^n \tag{7}$$

where C is a constant and determined to be zero by the following boundary condition (that is a result of symmetry):

$$\left.\frac{du}{dr}\right|_{r=0} = 0 \tag{8}$$

Note $\left|\frac{du}{dr}\right| = -\frac{du}{dr}$ for the capillary tube under consideration. Then (7) can be rewritten as

$$-\frac{du}{dr} = \left(\frac{dp}{dx}\right)^{1/n}\left(\frac{r}{2\kappa}\right)^{1/n} \tag{9}$$

Further, using non-slip conditions on the surface of the capillary tube ($u = 0$ at $r = R$), the solution to (9) is given as

$$\begin{aligned} u(r) &= \left(\frac{dp}{dx}\right)^{1/n}\int_R^r\left(\frac{r}{2\kappa}\right)^{1/n}dr \\ &= \left(\frac{dp}{dx}\right)^{1/n}\left(\frac{1}{2\kappa}\right)^{1/n}\frac{n}{n+1}\left[R^{1+\frac{1}{n}} - r^{1+\frac{1}{n}}\right] \end{aligned} \tag{10}$$

The above equation gives the velocity distribution along the radius direction. The average water flux across the cross-sectional area of the tube is then determined by

$$\begin{aligned} q_C &= \frac{\int_0^R u(r)(dr)(2\pi r)}{2\pi R^2} \\ &= \left(\frac{1}{2\kappa}\right)^{1/n}\frac{n(n+1)}{2(n+1)(3n+1)}R^{1+\frac{1}{n}}\left(\frac{dp}{dx}\right)^{\frac{1}{n}} \end{aligned} \tag{11}$$

2.3. Theoretical model for unsaturated clay materials

The pore space in a porous medium is often conceptualized as a group of capillary tubes with different tortuosity values and sizes (van Genuchten, 1980; Burdine, 1953). Thus, Eq. (11) for a single capillary tube can be extended to represent the relationship between water flux, q, and hydraulic gradient $\frac{dH}{dx}$ in porous media:

$$q = -K\left(\left|\frac{dH}{dx}\right|\right)^{\frac{1}{n}}i \tag{12}$$

where H is the hydraulic head, K is hydraulic conductivity, and i is the unit vector for hydraulic gradient. Note that for a single capillary tube, K is proportional to $R^{1+\frac{1}{n}}$, rather than R^2. (The latter is valid for Newtonian fluids corresponding to $n = 1$.) The relationship between hydraulic conductivity for a capillary tube and its radius R is the foundation for studying relative permeability under unsaturated conditions. Equations similar to (12) were reported by a number of researchers (e.g., Pascal, 1983; Wu and Pruess, 1998; Lopez et al., 2003). Most previous studies deal with single-phase fluid flow except Wu and Pruess (1998), who did not, however, consider how non-Newtonian behavior may affect unsaturated flow properties. As discussed below, the major focus of this study is on determining how non-Newtonian behavior impacts the unsaturated properties of clay materials.

For unsaturated media, capillary pressure P_c can be related to water saturation by the well-known Brooks and Corey (1964) relationship:

$$S_e = \left(\frac{P_c}{P_d}\right)^{-\lambda} \quad \text{for } P_c < P_d \tag{13.1}$$

$$S_e = 1 \quad \text{for } P_c \geqslant P_d \tag{13.2}$$

In (13), λ is a fitting factor related to pore-size distribution, P_d is the air entry value, and S_e is the effective saturation defined by

$$S_e = \frac{\theta - \theta_r}{\theta_s - \theta_r} \tag{14}$$

where θ, θ_s, and θ_r are water content, saturated water content, and residual water content, respectively.

In the literature, the relative permeability for unsaturated media has often been provided by the Burdine (1953) model:

$$K_r = \frac{K}{K_{sat}} = S_e^2\frac{\int_0^{S_e}P_c^{-2}dS_e}{\int_0^1 P_c^{-2}dS_e} \tag{15}$$

where K_{sat} is saturated hydraulic conductivity. In Eq. (15), S_e^2 represents tortuosity, and $\frac{1}{P_c}$ characterizes the size (or radius) of the capillary tube (or pore space) under saturation S_e. The power value of -2 in the two integrals results from the fact that, for Newtonian fluids, hydraulic conductivity for a capillary tube is proportional to the square of its radius. Therefore, Eq. (15) is valid for Newtonian fluid only, because for a non-Newtonian fluid, the hydraulic conductivity of a capillary tube is not proportional to the square of the radius. Based on Eq. (11), the Burdine (1953) model for a non-Newtonian fluid needs to be rewritten as:

$$K_r = \frac{K}{K_{sat}} = S_e^2\frac{\int_0^{S_e}P_c^{-(1+\frac{1}{n})}dS_e}{\int_0^1 P_c^{-(1+\frac{1}{n})}dS_e} \tag{16}$$

Combining Eqs. (13) and (16) yields

$$K_r = \left(\frac{P_c}{P_d}\right)^{-\left(\frac{1}{n}+1+3\lambda\right)} \tag{17}$$

and

$$K_r = S_e^{3+\frac{1+\frac{1}{n}}{\lambda}} \tag{18}$$

In deriving Eqs. (17) and (18), we assumed that pore geometry does not change with saturation or capillary pressure. The hydraulic conductivity change is purely a function of changes in saturation. In reality, clay swells (or shrinks) with changes in saturation. In this case, the relative conductivity is given by

$$K_r^* = \frac{K}{K_{ref}} = \left(\frac{K_r}{K_{ref,r}}\right)\left(\frac{K_{sat}}{K_{ref,sat}}\right) = \left(\frac{P_c P_{ref,d}}{P_d P_{ref,c}}\right)^{-\left(\frac{1}{n}+1+3\lambda\right)}\left(\frac{K_{sat}}{K_{ref,sat}}\right) \quad (19)$$

The subscript *ref* refers to the reference case in which measurements are available. For mechanically deformed media, it is convenient to define relative hydraulic conductivity respective to a reference case. In this case, relative conductivity can be larger than one. Also, in (19), we assumed, for simplicity, that pore-size distribution (or parameter λ) remains unchanged during swelling/shrinkage.

Based on the principle of Leverett (1941) scaling, relative changes in pore size can be approximately characterized by relative changes in porosity ϕ. By definition of air entry value P_d and using (11), we have:

$$\frac{P_{ref,d}}{P_d} = \frac{\phi}{\phi_{ref}} \quad (20)$$

$$\frac{K_{sat}}{K_{ref,sat}} = \left(\frac{\phi}{\phi_{ref}}\right)^{(1+\frac{1}{n})\alpha} \quad (21)$$

where parameter $\alpha > 1$ accounts for the fact that the porosity ratio may underestimate the corresponding size ratio for those well-connected pores that determine the hydraulic conductivity. Dixon et al. (1999) showed that $\alpha > 2.3$ for some saturated clay materials within a Darcian-flow regime.

Combining (19)–(21), we obtain

$$K_r^* = \left(\frac{P_c}{P_{ref,c}}\right)^{-\left(\frac{1}{n}+1+3\lambda\right)}\left(\frac{\phi}{\phi_{ref}}\right)^{(\alpha-1)\left(1+\frac{1}{n}\right)-3\lambda} \quad (22)$$

In the right-hand side of (22), the first and second terms represent conductivity changes resulting from changes in capillary pressure and swelling (shrinkage), respectively. The second term needs to be determined by measurements or estimated using geomechanical simulators. Eqs. (12), (13), and (22) give the constitutive relationships required for modeling unsaturated flow in clay materials. Their validity will be evaluated in the next section by examining their consistency with data.

3. Comparisons with experimental observations

As previously indicated, non-Darcian flow is a result of non-Newtonian properties of pore water in clay. However, experimental studies of non-Newtonian flow in porous media are very limited for unsaturated flow conditions. Most recently, Cui et al. (2008) reported on measurements of unsaturated hydraulic conductivity for a compacted sand-bentonite mixture. To the best of our knowledge, this work provided the first reliable data set of water flux as a function of hydraulic gradient under unsaturated conditions.

The tests of Cui et al. (2008) were conducted under two experimental boundary conditions: constant volume and free swelling. In this study, we focus on the data for constant-volume conditions only, based on the reasoning that under constant-volume conditions and for a given capillary pressure, hydraulic processes and pore structures are approximately the same at different locations within the soil sample (Cui et al., 2008). Experimental determinations of the flux–gradient relationships required the use of this approximation. Cui et al. (2008) used the instantaneous profile method to determine the unsaturated hydraulic conductivity for infiltration tests of a vertical sand–bentonite column. The sand–bentonite mixture was directly compacted in a metallic cylinder (50 mm in inner diameter, 250 mm high). The bottom of the test cell was connected to a water source, and the upper end to an air source under atmospheric pressure. Under transient water-flow conditions, vertical distributions of capillary pressure were directly measured as a function of time at several locations along the column. The relationship between water content and capillary pressure was independently measured under constant volume conditions. This relationship enables them to estimate vertical distributions of water content from the capillary-pressure measurements. Based on these vertical distributions at different times, and on the mass balance at each location within the soil column, they estimated the water flux at that location as a function of capillary pressure and hydraulic gradient. The details of this instantaneous method can be found in Cui et al. (2008).

Fig. 3 shows estimated water flux (data points) as a function of hydraulic gradient under several capillary pressures. Obviously, very strong nonlinear (non-Darcian) behavior emerges at all the different capillary pressures, indicating that Darcy's law is not valid for the range of hydraulic gradients under consideration. Based on Fig. 8 of Cui et al. (2008), the unit of hydraulic gradient in Fig. 3 is m/m. This seems to support the notion that non-Darcian flow behavior becomes more significant under unsaturated conditions. In unsaturated materials, pore water exists in water films or resides in relatively small pores, and therefore is subject to relatively strong interactions with the clay surface, as previously indicated.

Fig. 3 also matches Eq. (12) (solid lines) with data for the six capillary pressures. The single value of $n = 0.28$ is able to fit all the data points reasonably well. In general, n can be considered a measure of non-Newtonian behavior that may be saturation (or capillary pressure) dependent. Thus, n may also be a function of saturation in a general case. It appears that the data of Cui et al. (2008) support the use of a constant n for different capillary pressures—but more evaluations are needed before the issue can be fully resolved.

The solid curve in Fig. 4 shows the values for relative hydraulic conductivity defined in Eq. (19). The properties at capillary pressure of 35 MPa are used as reference properties. Thus, $K_r^* = 1$ in Fig. 4 at that capillary pressure. Note that for Darcian unsaturated flow in a rigid material, hydraulic conductivity always decreases with capillary pressure, which is not the case here. This underscores the importance of the fact that conventional unsaturated flow theory and methodology cannot be simply borrowed for clay materials. The data presented in Fig. 4 are from laboratory measurements reported by Cui et al. (2008). The flux and hydraulic gradient data provided by Cui et al. (2008)—the data needed to

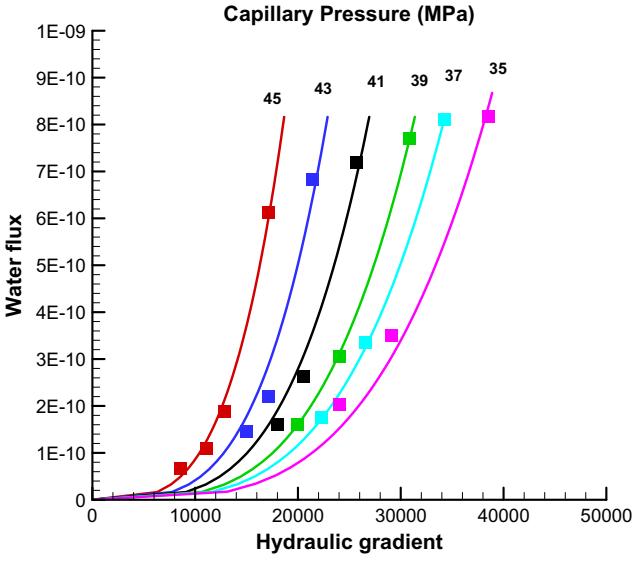

Fig. 3. Comparisons between calculated (solid curves) and estimated (data points) water flux (m/s) as a function of hydraulic gradient (m/m) for different capillary pressures. The calculation is based on Eq. (12).. Data from Cui et al. (2008)

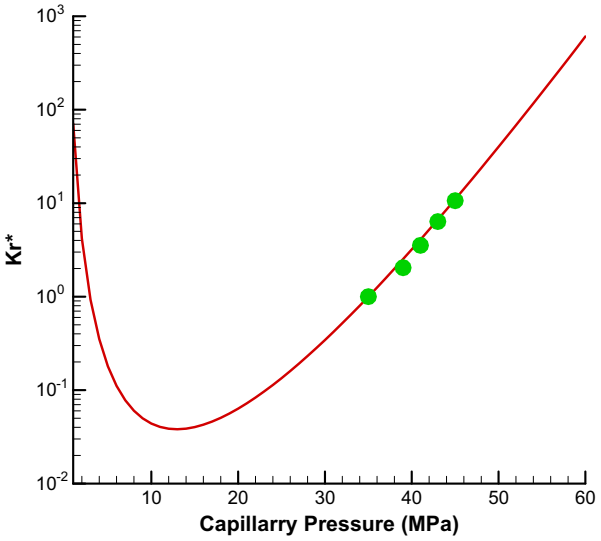

Fig. 4. Calculated unsaturated hydraulic conductivity as a function of capillary pressure. The data points are determined from Fig. 3. The solid curve is calculated from Eqs. (22) and (23) as an illustrative case. Unsaturated conductivity is defined in Eq. (19) with reference properties given at capillary pressure of 35 MPa. Data from Cui et al. (2008).

compute relative hydraulic conductivity—are limited to the capillary pressure range of the data points given in Fig. 4.

The observed relationship between hydraulic conductivity and capillary pressure can be explained with Eq. (22), in which the first and second terms represent conductivity changes resulting from changes in capillary pressure and swelling (shrinkage), respectively. For the observed range of capillary pressures, the effects of shrinkage (as a result of increasing capillary pressure) may dominate the changes in K_r^*. To further demonstrate our reasoning, assume that porosity and capillary pressure obey the following relationship:

$$\frac{\phi}{\phi_{ref}} = \exp\left[\beta\left(\frac{P_c}{P_{ref,c}} - 1\right)\right] \tag{23}$$

where β is a fitting factor. The above equation is based on the consideration that the amount of clay swelling seems to be an exponential function of capillary pressure (Pham et al., 2007), and that porosity change may be proportional to the amount of swelling (or shrinkage) under constant-volume conditions.

The solid curve in Fig. 4 is calculated using Eqs. (22) and (23) with $n = 0.28$ (obtained from Fig. 3), $\lambda = 0.21$ (obtained from Fig. 2 of Cui et al., 2008), $\alpha = 3.27$, and $\beta = 1.13$, and matches the observed conductivities. Note that K_r^* decreases with increasing capillary pressure for small levels of capillary pressure, and then increases with increasing capillary pressure for higher levels of capillary pressure. This is because for relatively small capillary pressures, the behavior of K_r^* is dominated by the first term on the right-hand side of Eq. (22); and for relatively large capillary pressures, the behavior of K_r^* is dominated by the second term, representing the effects of clay shrinkage. Although the definition of hydraulic conductivity in Cui et al. (2008) is different from ours, their results show similar behavior to the solid curve in Fig. 4. However, it is important to emphasize that the solid curve in the figure should be considered as an illustrative case, because the derivation of Eq. (23) requires some untested assumptions. The accurate determination of porosity change under test conditions of Cui et al. (2008) needs to be rigorously based on coupled hydro-mechanical processes. Nevertheless, comparisons between our theoretical results and data (Figs. 3 and 4) support the usefulness of our approach.

More experimental studies are needed to further confirm the non-Newtonian behavior and evaluate the proposed relationships for the unsaturated flow properties. Development of more efficient and applied experimental procedures is desirable for collecting relevant data sets. Along this line, it is useful to note that a commonly used method to estimate unsaturated soil properties for Newtonian fluids is the so-called Boltzmann transformation method (Bruce and Klute, 1956). It is based on a mathematical transformation of the partial differential equation describing unsaturated water flow in a horizontal soil column to an ordinary differential equation (ODE). Then water content (or saturation) data from the soil column are used to derive the unsaturated properties using the ODE. The appendix to this paper extends the method to non-Newtonian fluids, while swelling/shrinkage effects are not yet considered. Incorporation of these effects requires further study.

4. Concluding remarks

Unsaturated flow occurs over a period of time in the engineered barrier and in the near field of a clay repository for high-level radioactive waste. Therefore, accurately modeling unsaturated flow in clay materials is important for assessing the performance of a geological repository in isolating the radioactive waste. The non-Darcian behavior of water flow in clay materials has been demonstrated in the literature. While several models have been proposed for dealing with non-Darcian behavior for saturated flow conditions, a systematic study of modeling unsaturated non-Darcian flow is still lacking. Based on the hypothesis that pore water in clay becomes non-Newtonian as a result of water–clay interaction, we proposed constitutive relationships for unsaturated flow, including a relationship between water flux and hydraulic gradient and those among capillary pressure, water saturation, and hydraulic conductivity. An evaluation based on a set of laboratory experimental observations supports the usefulness of the proposed relationships.

Acknowledgments

The original version of this paper is reviewed by Dan Hawkes and Boris Faybishenco at Lawrence Berkeley National Laboratory, Prasad Nair from US Department of Energy, and Yifeng Wang and Kevin McMahon at Sandia National Laboratories. Their constructive comments are appreciated. We also appreciate comments from the Associate Editor and anonymous reviewers. This work was funded by and conducted for the Used Fuel Disposition Campaign under DOE Contract No. DE-AC02-05CH11231

Appendix A

Based on continuity, a flow equation describing the movement of water in a horizontal, semi-infinite unsaturated porous rock is given by:

$$\frac{\partial\theta}{\partial t} = -\frac{\partial q_x}{\partial x} \tag{A.1}$$

where θ is the volumetric moisture content, t is the time since start of test, x is the horizontal distance from inlet, and q_x is the water flux given by (12). Inserting (12) into (A.1) gives

$$\frac{\partial\theta}{\partial t} = \frac{\partial}{\partial x}\left[D(\theta)\left(\frac{\partial\theta}{\partial x}\right)^{\frac{1}{n}}\right] \tag{A.2}$$

where water diffusivity $D = K\left(\frac{\partial H}{\partial\theta}\right)^{\frac{1}{n}}$ is the moisture diffusivity. Eq. (A.2) can be reduced to an ordinary differential equation by incorporating a new Boltzmann transformation:

$$\lambda = xt^{\frac{-n}{n+1}} \tag{A.3}$$

Note that for an Newtonian fluid ($n = 1$), the power value in the above equation is –0.5. This value has been widely used in the literature of soil physics (Bruce and Klute, 1956). Combining (A.2) and (A.3) yields:

$$-\frac{n\lambda}{n+1}\frac{d\theta}{d\lambda} = \frac{d}{d\lambda}\left[D(\theta)\left(\frac{d\theta}{d\lambda}\right)^{\frac{1}{n}}\right] \tag{A.4}$$

To determine parameter n and water diffusivity from the above equation, water content data need to be collected from the soil column. In general, water is applied at one end of a long horizontal tube of air-dried or partially wet soil, at a small but constant pressure, and allowed to move into the soil column for a measured period of time. The column must be sufficiently long to be regarded as semi-infinite in length. Parameter n may be determined in such a way that the observed water content value is a function of λ only through adjusting the n value in (A.3). Once n is determined, the detailed procedure for estimating water diffusivity as a function of water content from measurements is available from Bruce and Klute (1956).

References

Barnichon, J.D., Volckaert, G., 2003. Observations and predictions of hydromechanical coupling effects in the Boom Clay, Mol underground research laboratory, Belgium. Hydrogeol. J. 11 (1), 193–202.

Brooks, R.H., Corey, A.T., 1964. Hydraulic properties for porous media. Hydro. Rep. No. 3, Colorado State University, Fort Collins.

Bruce, R.R., Klute, A., 1956. The measurement of soil moisture diffusivity. Soil Sci. Soc. Am. Proc. 20, 458–462.

Burdine, N.T., 1953. Relative permeability calculations from pore size distribution data. Am. Ins. Min. Metail. Pet. Eng 198, 71–77.

Christopher, R.H., Middleman, S., 1965. Power-law flow through a packed tube. I and EC Fundamentals 4 (4), 422–426.

Cui, Y.J., Tang, A.M., Loiseau, C., Delage, P., 2008. Determining the unsaturated hydraulic conductivity of a compacted sand-bentonite mixture under constant-volume and free-swell conditions. Phys. Chem. Earth 33, S462–S471.

Dixon, D.A., Graham, J., Gray, M.N., 1999. Hydraulic conductivity of clays in confined tests under low hydraulic gradients. Can. Geotech. J. 36, 815–825.

Fouche, O., Wright, H., Cleach, J.L., Pellenard, P., 2004. Fabric control on strain and rupture of heterogeneous shale samples by using a non-conventional mechanical test. Appl. Clay Sci. 26, 367–387.

Hansbo, S., 2001. Consolidation equation valid for both Darcian and non-Darcian flow. Geotechnique 51 (1), 51–54.

Leverett, M.C., 1941. Capillary behavior in porous solids. Trans. Am. Inst. Min. Metall. Eng. 142, 152–169.

Lopez, X., Valvatne, P.H., Blunt, M.J., 2003. Predictive network modeling of single-phase non-Newtonian flow in porous media. J. Colloid Interface Sci. 264, 256–265.

Low, P.F., 1961. Physical chemistry of clay–water interaction. Adv. Agron. 13, 269–327.

Meier, P., Trick, T., Blumling, P., Volckaert, G., 2000. Self-Healing of Fractures within the EDZ at the Mont Terri Rock Laboratory: Results after One Year of Experimental Work. In: Proceedings of the International Workshop on Geomechanics, Hydromechanical and Thermomechanical Behavior of Deep Argillaceous Rocks: Theory and Experiments, Paris, October 11–12, 2000.

Pascal, H., 1983. Rheological behavior effect of non-Newtonian fluids on steady and unsteady flow through a porous medium. Int. J. Numer. Anal. Meth. Geomech. 7, 289–303.

Patriarche, D., Ledoux, E., Simon-Coincon, R., Michelot, J., Cabrera, J., 2004. Characterization and modeling of diffusive process for mass transport through the tournemire argillites Aveyron, France. Appl. Clay Sci. 26, 109–122.

Pham, Q.T., Vales, F., Malinsky, L., 2007. Effects of desaturation-resaturation on mudstone. Phys. Chem. Earth Parts A/B/C 32 (8–14), 646–655.

Van Genuchten, M., 1980. A closed-form equation for predicting the hydraulic conductivity of unsaturated soil. Soil. Sci. Soc. Am. J. 44 (5), 892–898.

Wu, Y.S., Pruess, K., 1998. A numerical method for simulating non-Newtonian fluid flow and displacement in porous media. Adv. Water Resour. 2, 351–362.

Zou, Y., 1996. A non-linear permeability relation depending on the activation energy of pore liquid. Geotechnique 46 (4), 769–774.